Astron. Astrophys. 359, 483–488 (2000)

ASTRONOMY
AND
ASTROPHYSICS

Dense gas in the dust lane of Centaurus A⋆

W. Wild[1] **and A. Eckart**[2]

[1] Kapteyn Institute, University of Groningen, Landleven 12, P.O. Box 800, 9700 AV Groningen, The Netherlands
[2] Universität zu Köln, I. Physikalisches Institut, Zülpicherstrasse 77, 50937 Köln, Germany

Received 16 February 2000 / Accepted 4 May 2000

Abstract. The interstellar medium of Centaurus A (NGC 5128) has been studied extensively in recent years, using mostly molecular lines tracing low to medium density gas (500 to several 10^3 cm^{-3}). The amount and distribution of the dense molecular gas was largely unknown. Here we present new millimeter data of the HCN(1–0), CS(2–1), and CS(3–2) rotational transitions towards the nearby radio galaxy Centaurus A observed with the SEST on La Silla, Chile. We obtained spectra of the HCN(1–0) emission which traces dense 10^4 cm^{-3} molecular gas at the center and along the prominent dust lane at offset positions $\pm 60''$ and $\pm 100''$. We also obtained a few spectra of CS(2–1) and (3–2) tracing densities of $\sim 10^5$ cm^{-3}. The emission in these lines is weak and reaches a few mK at the available angular resolutions of $54''$ - $36''$. At the central position, the integrated intensity ratio I(HCN)/I(CO) peaks at 0.064, and decreases to $\sim$0.02 to 0.04 in the dust lane.

Using the new high density tracer data, we estimate the amount, distribution and physical conditions of the dense molecular gas in the dust lane of Centaurus A. We find that Cen A and the Milky Way are comparable in their HCN(1-0) line luminosity. However, towards the nucleus the fraction of dense molecular gas measured via the line luminosity ratio L(HCN)/L(CO) as well as the star formation efficiency $L_{\rm FIR}/L_{\rm CO}$ is comparable to ultra-luminous infrared galaxies (ULIRGs). Within the off-nuclear dust lane and for Cen A as a whole these quantities are between those of ULIRGs and normal and infrared luminous galaxies. This suggests that most of the FIR luminosity of Centaurus A originates in regions of very dense molecular gas and high star formation efficiency.

Key words: galaxies: nuclei – galaxies: individual: Cen A, NGC 5128 – galaxies: ISM – radio lines: galaxies – radio lines: ISM – ISM: molecules

1. Introduction

Centaurus A (NGC 5128) is the closest radio galaxy (distance 3.5 Mpc, $1'' = 17$ pc, Soria et al. 1996, Hui et al. 1993, Israel 1998, Ebneter & Balick 1983, de Vaucouleurs 1979) and exhibits a very prominent dust lane. Centaurus A is a strong radio galaxy with a milliarcsecond nuclear continuum source (Kellermann et al. 1997; Shaffer & Schilizzi 1975; Kellermann 1974) and two giant radio lobes. Absorption against the nuclear source has been found in HI (van der Hulst et al. 1983) and many molecular species and transitions (Gardner & Whiteoak 1976; Whiteoak & Gardner 1971; Bell & Seaquist 1988; Seaquist & Bell 1986, 1990; Phillips et al. 1987; Eckart et al. 1990a; Israel et al. 1990, 1991; Wild et al. 1997; Wiklind & Combes 1997).

Several studies of Centaurus A in the millimeter wavelength range have been carried out. Although other elliptical galaxies with dust lanes have recently been detected in CO (Sage & Galleta 1993), Centaurus is the best object for a detailed study due to its proximity and corresponding large angular size. Phillips et al. (1987) and Quillen et al. (1992) observed several positions in the CO(2-1) line along the dust lane at a resolution of $30''$. In previous papers we presented a fully sampled map of the ^{12}CO(1-0) emission together with *IRAS* observations of the FIR continuum (Eckart et al. 1990b), measurements of the millimeter absorptions lines towards the nucleus (Eckart et al. 1990a; see also Wiklind & Combes 1997), and a ^{12}CO(2-1) map along the dust lane at a resolution of $22''$ (Rydbeck et al. 1993).

In Wild et al. (1997) we presented the first fully sampled ^{13}CO(1-0) map along the dust lane of Centaurus A, as well as single spectra of the ^{13}CO(2-1) emission in the disk and C^{18}O(1-0) emission at the central position. These new data allowed us, in combination with the ^{12}CO(1-0) and ^{12}CO(2-1) maps obtained earlier, to study the excitation conditions of the molecular gas in detail throughout the dust lane. Using different CO line ratios and their variation across the disk of Centaurus A, we inferred the physical parameters of the molecular ISM and their spatial variations.

Here we extend our investigation to the very dense (10^4 to 10^5 cm^{-3}) phase of the molecular gas by observing line emission of the density tracers HCN and CS towards the nucleus and the off-nuclear dust lane in Centaurus A.

2. Observations

The observations were carried out in two observing runs in January 1996 and January 1998 with the 15m Swedish ESO Submillimeter Telescope (SEST) on La Silla, Chile. The adopted central position for Centaurus A was $\alpha(1950) = 13^h22^m31.8^s$ and $\delta(1950) = -42°45'30''$. We observed the ^{12}CO(1-0),

Send offprint requests to: W. Wild (wild@astro.rug.nl)

⋆ Based on observations collected at the European Southern Observatory, La Silla, Chile

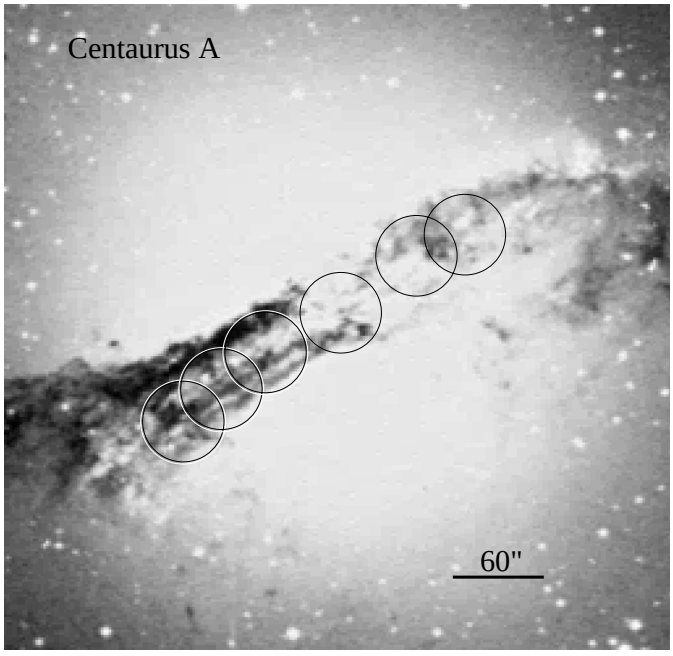

Fig. 1. Beam positions at which the dense molecular gas in the dust lane of Centaurus A has been investigated. Shown is the beam for the HCN J=1–0 measurements.

HCN(1-0), CS(2-1), and CS(3-2) molecular line emission and absorption towards the central non-thermal continuum source and selected positions in the dust lane. We used the 3 mm and 2 mm SIS receivers with system temperatures around 140 K and 180 K, respectively, and beam widths ranging from 34″ (FWHM) at 147 GHz to 56″ at 89 GHz. We observed in the dual beam switching mode, i.e. a chopper wheel switched between two positions on the sky displaced by about 12 arcminutes in azimuth. First the source was placed in one beam and then in the other beam. The backend was the low resolution acousto-optical spectrometer with a bandwidth of about 1 GHz in 1440 channels. The separation between channels was 0.7 MHz, and the actual spectral resolution 1.4 MHz (4.7 km s^{-1} at 89 GHz). We adopted the LSR velocity scale. The system was flux calibrated with the chopper wheel method (Kutner & Ulich 1981). We used main beam efficiencies $\eta_{\rm MB,89GHz}$ = 0.75, $\eta_{\rm MB,97GHz}$ = 0.73, $\eta_{\rm MB,115GHz}$ = 0.70, and $\eta_{\rm MB,147GHz}$ = 0.66 for the conversion from antenna temperature to Rayleigh-Jeans main beam brightness temperatures. The pointing was accurate to within 3″. It was checked frequently on the nuclear continuum source of Centaurus A, and the nearby (distance $\sim$ 17°) SiO maser W Hya. Fig. 1 shows the positions in the dust lane of Centaurus A at which the dense molecular gas has been investigated. Fig. 2 and Fig. 3 show the HCN J=1–0 and CS spectra along the dust lane. Table 1 gives parameters of the observed spectra.

3. Analysis

In order to measure the mass of dense molecular gas and therefore the star formation potential in the dust lane of Centaurus A we observed HCN and CS line emission. Both molecules trace higher density gas than CO, since they have large dipole moments and require n(H$_2$)$\geq$10^4 cm^{-3} for significant excitation. The analysis is done by calculating the line luminosities and estimating from them the amount of dense molecular gas. These properties are then discussed and compared to data from the Milky Way and external galaxies.

Table 1. Observational parameters

Transition	offset RA, Dec (arcsec)	integration time (min)	$T^*_{\rm A,max}$ (mK)	Δv (km s^{-1})
HCN(1-0)	+105,-73	178	<2.0	
	+79,-55	460	4.0	230
	+50,-25	396	5.0	190
	0,0	252	8.5	390
	-52,+37	836	3.8	170
	-79,+55	360	4.0	170
CS(3-2)	+50,-25	1644	0.9	250
	0,0	712	3.8	105
CS(2-1)	-52,+37	288	3.0	135

Line luminosities can be obtained from the integrated line intensities $I_{\rm line} = \int T_{\rm MB} \times \delta v$ via

$$L_{\rm line} = I_{\rm line}\, D^2\, \Omega \ , \qquad (1)$$

where $T_{\rm MB}$ is the main beam brightness temperature, D is the distance to the source and Ω is the solid angle of the beam convolved with the source.

Using radiative transfer solutions (e.g. Kwan & Scoville 1975, Linke & Goldsmith 1980), assuming that the HCN and CS line emission traces gravitationally bound or virialized clouds with a density range of a few 10^4 cm^{-3} to a few 10^5 cm^{-3} and kinetic temperatures between 10 to 60 K. Solomon et al. (1990, 1992) present relations between the mass of molecular gas at these densities and the corresponding observed line luminosity as defined above. For HCN(1-0) they find in their 1992 paper

$$M_{\rm HCN} \sim 20^{+30}_{-10} \times L_{\rm HCN} \quad {\rm M}_\odot\ ({\rm K\ km\ s^{-1}})^{-1} \qquad (2)$$

and for CS(2-1) they derive in the 1990 paper

$$M_{\rm CS} \sim (35-150) \times L_{\rm CS} \quad {\rm M}_\odot\ ({\rm K\ km\ s^{-1}})^{-1} \ . \qquad (3)$$

The assumptions made above are likely to be valid for the molecular ISM in Centaurus A as well. This can be based on the fact that, according to radiative transport calculations (Eckart et al. 1990a), the lower density molecular gas - as traced by CO isotopic emission - has similar properties compared to those in Galactic GMCs and galaxies with indications for enhanced star formation activity.

Although the mass estimates derived using the relations given above include considerable uncertainties they can be used as a general guide line to investigate the properties of the dense interstellar medium. The assumed kinetic temperature range appears to be appropriate for the dense star forming ISM in Centaurus A. Eckart et al. (1990b), Joy et al. (1988), as well as Marston & Dickens (1988) give dust temperatures in the dust

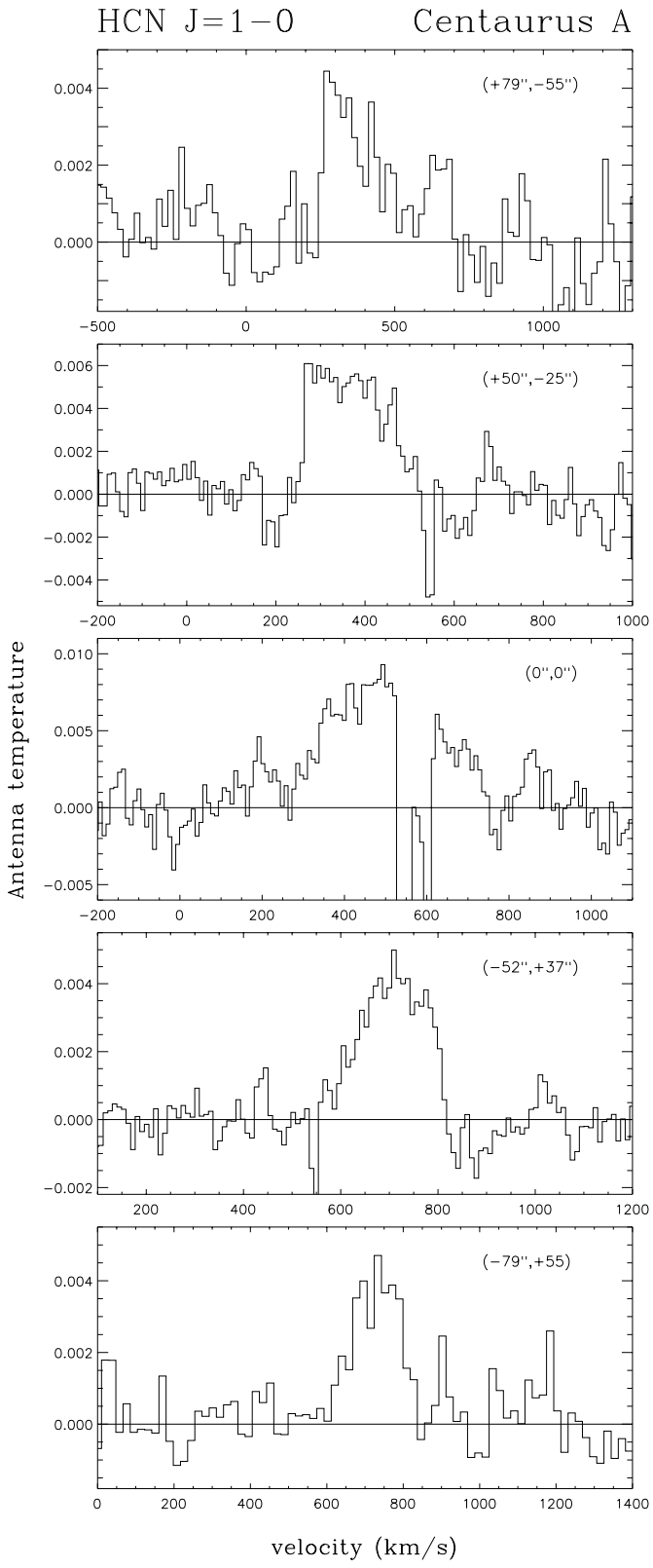

Fig. 2. HCN J=1–0 spectra along the dust lane of Centaurus A. Offsets are given relative to the center position $\alpha(1950) = 13^h22^m31.8^s$, $\delta(1950) = -42°45'30''$

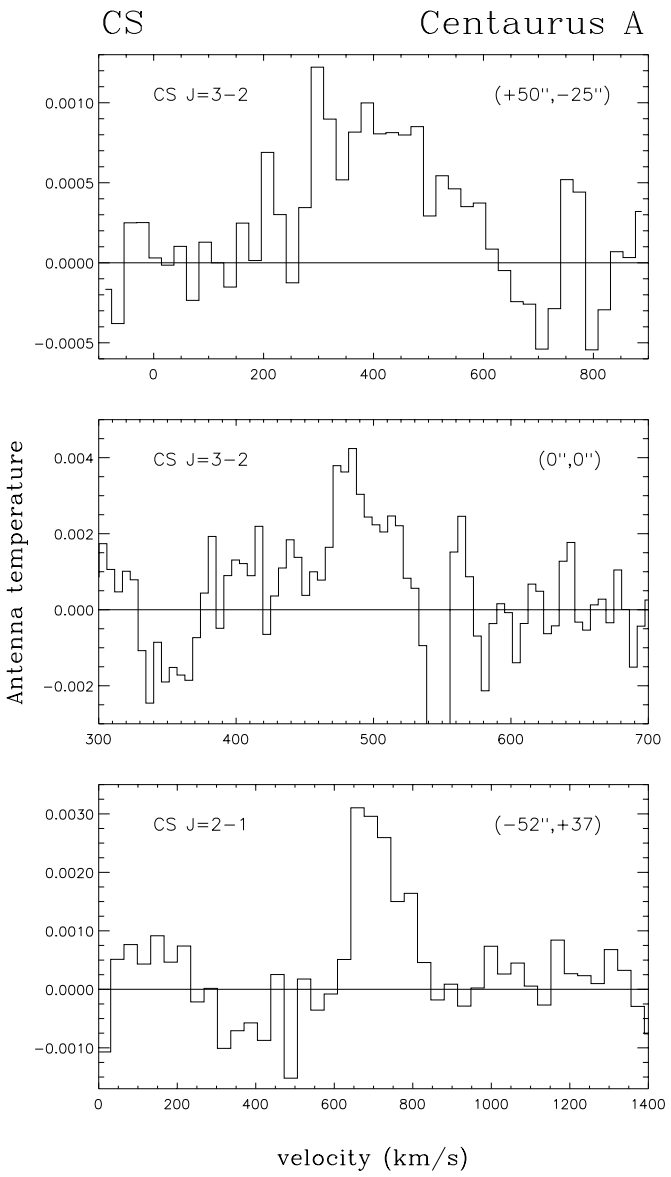

Fig. 3. CS J=3–2 and J=2–1 spectra along the dust lane of Centaurus A. Offsets are given relative to the center position $\alpha(1950) = 13^h22^m31.8^s$, $\delta(1950) = -42°45'30''$

lane in the range of 40 K. From the HCN(1-0)/HNC(1-0) ratio of about 2, Israel (1992) introduces kinetic temperatures of the order of ∼25 K.

Table 2 lists the integrated line intensities $\int T_{\rm MB} \times \delta v$ for the HCN(1-0) and the CO(1-0) line emission, as well as the ratios I(HCN)/I(CO) corrected for main beam efficiencies. In Table 3 we list the CO(1-0) and HCN(1-0) line luminosities as well as the estimated FIR luminosities $L_{\rm FIR}$ as a function of position and as estimated quantities integrated over the dust lane. Table 4 lists line intensities $\int T_{\rm MB} \times \delta v$ and luminosities (corrected for main beam efficiency) for CS(2-1) and CS(3-2) lines we measured at a few positions. Table 5 lists the mass of dense molecular gas as derived from the line luminosities and Eqs. (2) and (3).

Table 2. HCN/CO Line Ratios in Centaurus A

offset (RA, Dec) (arcsec)	distance from center (arcsec)	I(CO) (K km s^{-1})	I(HCN) (K km s^{-1})	$\frac{\mathrm{I(HCN)}}{\mathrm{I(CO)}}$
+105, -73	128	16.4	<0.40	<0.024
+79, -55	96	34.4	1.27	0.037
+50, -25	56	63.1	1.27	0.020
0, 0	0	69.0	4.40	0.064
-52, +37	-64	50.1	0.85	0.017
-79, +55	-96	27.3	0.91	0.033

Intensities are given in $\int T_{\mathrm{MB}} \times \delta v$.
Last column gives ratios. The assumed main beam efficiencies are $\eta_{\mathrm{MB,89GHz}}$=0.75 and $\eta_{\mathrm{MB,115GHz}}$=0.70.

Table 3. CO, HCN, and FIR luminosities

distance from center (arcsec)	$\mathrm{L_{CO}}$ 10^6(L$_\odot$)	$\mathrm{L_{HCN}}$ 10^6(L$_\odot$)	$\mathrm{L_{FIR}}$ 10^9 L$_\odot$	$\frac{\mathrm{L_{FIR}}}{\mathrm{L_{CO}}}$	$\frac{\mathrm{L_{HCN}}}{\mathrm{L_{CO}}}$
128	7.5	<0.31	0.6	80	<0.04
96	15.7	1.00	0.6	38	0.06
56	29.0	1.00	1.2	41	0.03
0	31.7	3.47	1.8	57	0.11
-64	23.0	0.67	1.2	52	0.03
-96	12.5	0.72	0.6	48	0.06
total	92	52	6.0	65	0.06

$L_{\mathrm{I}} = (\mathrm{K\ km\ s^{-1}})^{-1}\ \mathrm{pc}^2$
Intensities are given in $\int T_{\mathrm{MB}} \times \delta v$. The assumed main beam efficiencies are $\eta_{\mathrm{MB,89GHz}}$=0.75 and $\eta_{\mathrm{MB,115GHz}}$=0.70.

Table 4. CS line intensities and luminosities

distance from ctr (arcsec)	$I_{\mathrm{CS(2-1)}}$ K km s^{-1}	$I_{\mathrm{CS(3-2)}}$ K km s^{-1}	$L_{\mathrm{CS(2-1)}}$ $10^5 L_{\mathrm{I}}$	$L_{\mathrm{CS(3-2)}}$ $10^5 L_{\mathrm{I}}$
56		0.33		0.9×10^5
0		0.61		1.7×10^5
-64	0.55		3.5×10^5	
total			–	5.4×10^5

Intensities are given in $\int T_{\mathrm{MB}} \times \delta v$ corrected for $\eta_{\mathrm{MB,147GHz}}$=0.66 and $\eta_{\mathrm{MB,97GHz}}$=0.73.
Line luminosities are given in $L_{\mathrm{I}} = (\mathrm{K\ km\ s^{-1}})^{-1}\ \mathrm{pc}^2$.
The total CS(3-2) line luminosity has been derived assuming that the off-center measurements are representative for all of the dust lane which is 180″ in length in the CO(1-0) map (Eckart et al. 1990a).

4. Results and discussion

4.1. Dense gas traced by HCN

HCN traces molecular gas at much higher density of about $\sim10^4$ cm^{-3} than CO ($\sim$500 cm^{-3}). In Cen A the HCN emission within the dust lane is clearly detected over a similar velocity range as CO (v_{LSR}=250–850 km s^{-1}). The HCN emission, however, is stronger peaked on the nucleus compared to the CO emission. In Fig. 4 we compare the spatial variation of the intensity ratio I(HCN)/ I(CO) as it is observed in Cen A and M 51 (Kohno et al. 1996). At the central position, the integrated intensity ratio I(HCN)/ I(CO) peaks at 0.06, and decreases to $\sim$0.02 to 0.04 in the dust lane. Ratios of the order of 0.1 or higher are only observed in active nuclear regions of Seyfert galaxies and ULIRGs (Kohno et al. 1996; Solomon et al. 1992; Nguyen-Q-Rieu et al. 1992; Helfer & Blitz 1993, 1995; Jackson et al. 1993; Tacconi et al. 1994; Sternberg et al. 1994).

The ratio of HCN to CO luminosity is 1/6 for ULIRGs, but only 1/80 in normal spirals (Solomon et al. 1992). For Cen A the HCN to CO luminosity is $L_{\mathrm{CO}}/L_{\mathrm{HCN}}$=1/13 and therefore closer to the value for ULIRGs than normal spirals.

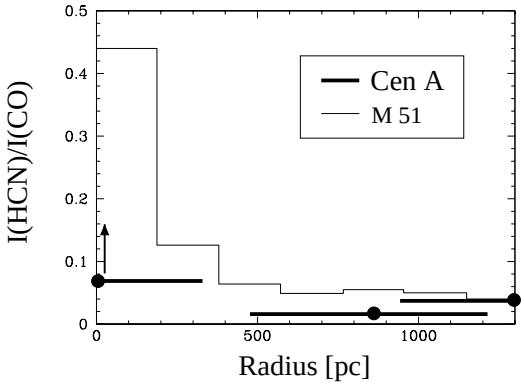

Fig. 4. Comparison of the HCN(1-0) to CO(1-0) line intensity ratio in M51 (Kohno et al. 1996) and Cen A as a function of position. The central ratio in Cen A is of the order of 0.1. Assuming than the HCN(1-0) line emission is concentrated on the nucleus the HCN(1-0) to CO(1-0) line intensity ratio will probably rise (as indicated by the arrow) if high angular resolution interferometric observations become possible.

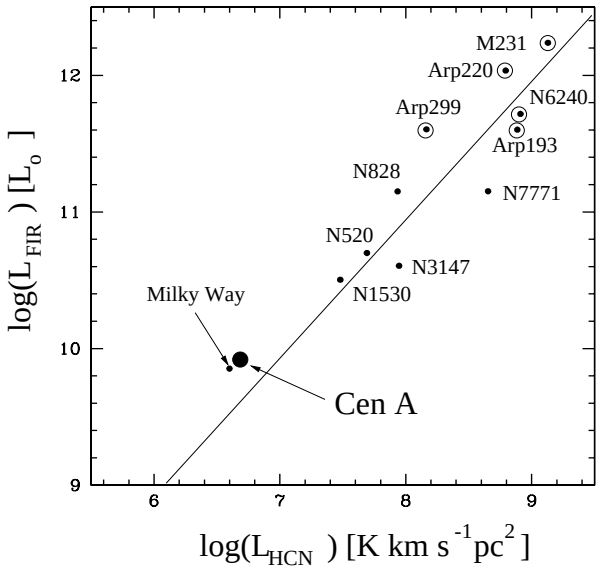

Fig. 5. Centaurus A has the same ratio of FIR to HCN luminosity as ULIRGs (dots in circles) and normal spirals (simple dots; Solomon et al. 1992). In both quantities Cen A and the Milky Way are very similar.

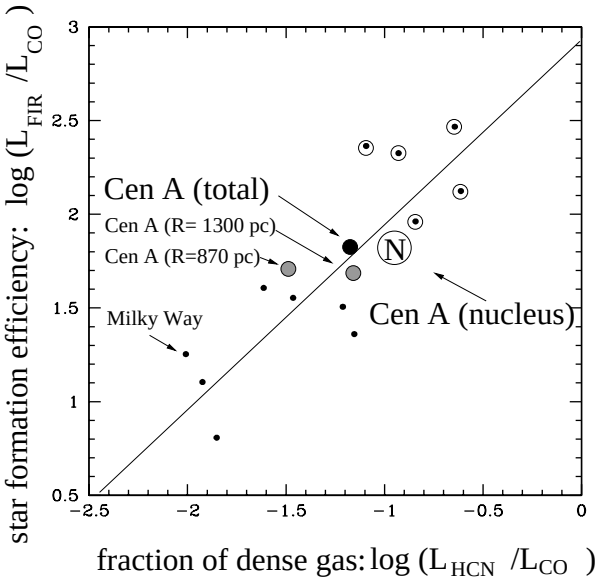

Fig. 6. Comparison of the fraction of dense gas to the star formation efficiency (Solomon et al. 1992). The nucleus of Cen A has properties of ULIRGS and the bulk of the dust lane falls between ULIRGS and normal or interacting galaxies. Symbols are the same as in Fig. 5.

Table 5. Dense molecular gas mass traced by HCN and CS

distance from center (arcsec)	$M_{\rm HCN}(H_2)$ $10^7 M_\odot$	$M_{\rm CS}(H_2)$ $10^7 M_\odot$
128	<0.6	
96	2.0	
56	2.0	0.8
0	4.3	1.6
-64	1.3	
-96	1.4	
total	8.6	5.0

Masses have been derived via line luminosities and Eqs. (2) and (3). Systematic errors are +150% and -50% for $M_{\rm HCN}(H_2)$ and $\pm$40% for $M_{\rm CS}(H_2)$. The total masses have been derived assuming that the off-center measurements are representative for all of the dust lane which is 180″ in length in the CO(1-0) map (Eckart et al. 1990a).

Fig. 5 shows that Centaurus A has the same ratio of FIR to HCN luminosity as ULIRGs and normal spirals, including the Milky Way. This is also true for the center and the off-positions in the dust lane. This suggests that in Cen A the star formation rate per mass of *dense* gas is in good approximation independent on the position and infrared luminosity within the dust lane.

Detailed observations (Lee et al. 1990) of Galactic GMC's show that the average CS(2-1)/CO(1-0) intensity ratio is ∼1/300. Since HCN(1-0) is usually 1.5 to 2 times stronger than CS(2-1) and has larger source sizes Solomon et al. (1992) adopt an HCN(1-0)/CO(1-0) ratio of ∼1/100 for the molecular ring in the Galactic disk. This results in a HCN luminosity for the Milky Way of about 4×10^6 K km s^{-1} pc^2 which is quite comparable to what we find for Centaurus A with 5.5×10^6 K km s^{-1} pc^2.

In Fig. 6 we show the position of Centaurus A in a plot of $log(L_{\rm HCN}/L_{\rm CO})$ which measures the fraction of dense gas and $log(L_{\rm FIR}/L_{\rm CO})$ which measures the efficiency with which molecular gas is transformed into OB stars (Solomon et al. 1992). This plot includes ULIRGs as well as normal and infrared luminous galaxies. We find that as a whole Cen A fits very well into this correlation and is located between both groups. This is also true for the disk at angular separations of about 60″ and 90″ from the center. However, towards the nucleus the fraction of dense molecular gas measured via the line luminosity ratio L(HCN)/L(CO) as well as the star formation efficiency $L_{\rm FIR}/L_{\rm CO}$ is more comparable to ULIRGs rather than normal and infrared luminous galaxies. This suggests that most of the FIR luminosity of Centaurus A originates in regions of very dense molecular gas and high star formation efficiency.

The HCN line luminosity can now be used to estimate the amount of dense (10^4 cm^{-3}) gas via Eq. (2). From the HCN line luminosity we find a total mass of molecular gas that must be at densities $>10^4$ cm^{-3} of $8.6^{+13}_{-4}\times10^7 M_\odot$. This has to be compared to the total molecular gas mass derived from the ^{12}CO(1-0) line of $2\times10^8 M_\odot$ (Eckart et al. 1990a). The comparison shows that a large fraction - approximately one third - but at least one sixth - of the molecular line emission in Cen A must originate from sites with abundant dense molecular gas. The ratio of molecular gas mass at densities of $>10^4$ cm^{-3} to gas at ∼300 cm^{-3} is about 1/20 in the Galaxy and almost unity for ULIRGs (Solomon et al. 1992). Based on this quantity the physical conditions of the dense molecular ISM in Cen A are apparently closer to those of ULIRGs than to our Milky Way. The presence of a large amount of dense molecular gas is also supported by the fact that if one multiplies $M_{\rm HCN}(H_2)$ by the mean Galactic $L_{\rm FIR}/M_{\rm HCN}(H_2)$ ratio of 71 $M_\odot({\rm K\,km\,s^{-1}})^{-1}$ pc^2 (Solomon et al. 1992) one obtains about $6\times10^9 L_\odot$ which equals the observed FIR luminosity. The implicite assumption here is that the mean Galactic conversion factor is applicable. Accepting this, the result implies that active star formation in the dust lane of Cen A is the actual source of its FIR luminosity and that the AGN which is responsible for strong radio and X-ray radiation is not contributing substantially.

4.2. Dense gas traced by CS

The CS(2-1) and CS(3-2) lines trace even denser molecular gas at 10^5 cm^{-3}. The problem is that CS line emission is quite weak. Detections of CS in extra-galactic sources are sparse. In the sample of normal and interacting galaxies and ULIRGs Solomon et al.(1992) detected CS line emission only in Arp 220. For Cen A we find a total CS(3-2) line luminosity of $L_{\rm CS(3-2)} \sim 5.4\times10^5$ K km s^{-1} pc^2. The ratio of the CS to CO line luminosity is then $L_{\rm CS(3-2)}/L_{\rm CO} \sim 1/170$, very similar to the value of 1/250 given by Solomon et al. (1990) for the Milky Way. For the Galactic Center the same authors derive a corresponding ratio of about 1/20 to 1/30. This indicates that the Galactic Center is approximately 8 to 10 times more luminous in the CS(3-2) line that the molecular gas in the disk. At

the center of Cen A the $L_{\mathrm{CS}(3-2)}$ is 2 times higher compared to the off-center dust lane measurement.

The CS(3-2) line luminosity results in a total mass estimate of gas at densities of 10^5 cm^{-3} of about $M_{\mathrm{CS}(3-2)}(H_2)$ = (2-8)$\times 10^7 \mathrm{M}_\odot$. This number is in very good agreement with the corresponding value derived from the HCN(1-0) line emission.

5. Conclusion

While the line luminosities of the HCN(1-0) and CS(3-2) as well as the FIR luminosity of the molecular gas in the dust lane of Cen A are quite comparable to each other there are definite differences in the overall fraction of dense molecular gas and the efficiency with which stars are formed from it. This star formation activity is also the source of the FIR luminosity of Cen A. About 40% or even more of the total molecular line luminosity in Cen A originates in dense gas. This suggests that star formation as well as the bulk of the dense molecular gas is mostly concentrated in GMC complexes rather than in a more diffuse molecular gas component. This is already indicated by the ring-like distribution of HII region found by Graham (1979) as well as the MEM deconvolved ^{12}CO(2-1) line emission mass by Rydbeck et al. (1993).

We also note that with respect to other positions in the dust lane the I(HCN)/I(CO) ratio is larger at separations of about 100″ from the nucleus rather than at separations of about 60″. The larger distance is close to the inner edge of the ring of HII regions and corresponds well with the position of the folds in the warped molecular gas disk of Centaurus A (Quillen et al. 1992, 1993; Sparke 1996) and an increased intensity in the 15 μm continuum dust emission (Block & Sauvage 2000; Mirabel et al. 1999). Therefore a higher I(HCN)/I(CO) ratio may be due to a combination of enhanced star formation efficiency at these positions and an increase in column density due to the folds. Due to the low intrinsic velocity dispersion of the thin molecular disk (Quillen et al. 1992) and due to the fact that the ^{12}CO line emission is originating in optically thick molecular gas (Wild et al. 1997) this may lead to shadowing of molecular clouds along the line of sight toward the folds. This effect will be stronger for ^{12}CO than for the small, dense cloud cores seen in the less abundant HCN line emission. This effect may therefore lead to an intensity decrease in the ^{12}CO line and an increase in the HCN(1-0) line, resulting in the observed variation of the I(HCN)/I(CO) line ratio.

Future interferometric measurements will allow us to study the distribution of molecular gas in the dust lane of Centaurus A in much greater detail. Line ratios, luminosities and star formation can then be investigated for individual GMC complexes.

Acknowledgements. We are grateful to the SEST team and the ESO staff on La Silla and in Garching for their support and hospitality. We thank Lars-Åke Nyman for taking an additional central CO spectrum.

References

Bell M.B., Seaquist E.R., 1988, ApJ 329, L17
Block D.L., Sauvage M., 2000, A&A 353, 72
Ebneter K., Balick B, 1983, PASP 95, 675
Eckart A., Cameron M., Genzel R., Jackson J., Rydbeck G., 1990a, ApJ 365, 522
Eckart A., Cameron M., Rothermel H., et al., 1990b, ApJ 363, 451
Gardner F.F., Whiteoak J.B., 1976, Proc. Astron. Soc. Aust. 3, 63
Graham J.A., 1979, ApJ 232, 60
Helfer T.T., Blitz L., 1993, ApJ 419, 86
Helfer T.T., Blitz L., 1995, ApJ 450, 90
Hui X., Ford H.C., Ciardullo R., Jacoby G.H., 1993, ApJ 414, 463
van der Hulst J.M., Golish W.F., Hashick A.D., 1983, ApJ 264, L37
Israel F.P., 1992, A&A 265, 487
Israel F.P., 1998, A&AR 8, 237
Israel F.P., van Dishoeck E.F., Baas F., et al., 1990, A&A 227, 342
Israel F.P., van Dishoeck E.F., Baas F., de Graauw Th., Phillips T.G., 1991, A&A 245, L13
Jackson J.M., Paglione T.A.D., Ishizuki S., Nguyen-Q-Rieu, 1993, ApJ 418, L13
Joy M., Lester D.F., Harvey P.M., Ellis H.B., 1988, ApJ 326, 662
Kellermann K.I., 1974, ApJ 194, L135
Kellermann K.I., Zensus A., Cohen M.H., 1997, ApJ 475, L93
Kohno K., Kawabe R., Tosaki T., Okumura S.K., 1996, ApJ 461, L29
Kutner M.L., Ulich B.L., 1981, ApJ 250, 341
Kwan J., Scoville N., 1975, ApJ 195, L85
Lee Y., Snell R.L., Dickman R.L., 1990, ApJ 355, 536
Linke R.A., Goldsmith P.F., 1980, ApJ 235, 437
Marston A.P., Dickens R.J., 1988, A&A 193, 27
Mirabel I.F., Laurent O., Sanders D.B., 1999, A&A 341, 667
Nguyen-Q-Rieu, Jackson J.M., Henkel C., Truong B., Mauersberger R., 1992, ApJ 399, 521
Phillips T.G., Ellison B.N., Keene J.B., et al., 1987, ApJ 322, L73
Quillen A.C., de Zeeuw P.T., Phinne E.S., Phillips T.G., 1992, ApJ 391, 121
Quillen A.C., Graham J.R., Frogel J.A., 1993, ApJ 412, 550
Rydbeck G., Wiklind T., Cameron M., et al., 1993, A&A 270, L13
Sage L., Galleta G., 1993, ApJ 419, 544
Seaquist E.R., Bell M.B., 1986, ApJ 303, L67
Seaquist E.R., Bell M.B., 1990, ApJ 364, 94
Shaffer D.B., Schilizzi R.T., 1975, ApJ 80, 753
Sparke L.S., 1996, ApJ 473, 810
Soria R., Mould J.R., Watson A.M., et al., 1996, ApJ 465, 79
Solomon P.M., Radford S.J.E., Downes D., 1990, ApJ 348, L53
Solomon P.M., Downes D., Radford S.J.E., 1992, ApJ 387, L55
Sternberg A., Genzel R., Tacconi L., 1994, ApJ 436, L131
Tacconi L.J., Genzel R., Blietz M. et al., 1994, ApJ 426, L77
de Vaucouleurs G., 1979, AJ 84, 1270
Whiteoak J.B., Gardner F.F., 1971, ApJ 8, L57
Wiklind T., Combes F., 1997, A&A 324, 51
Wild W., Eckart A., Wiklind T., 1997, A&A 322, 419